Journal of Engineering Science and Technology
Vol. 13, No. 9 (2018) 2685 - 2699

INVESTIGATION OF HALF-TONE MOTTLE IN COATED PAPERS BY VARYING GRAVURE PROCESS PARAMETERS

AKSHAY V. JOSHI

Department of Printing Engineering, P. V. G's College of Engineering and Technology, 44, Vidyanagari, Parvati, Pune, 411009, India
E-mail: joshiakshay1973@gmail.com

Abstract

Half-tone mottle is due to uneven ink transfer and ink penetration, which generates an inhomogeneous image to the human eye, thereby affecting the saleability of the product. Design of Experiments (DOE) was done with gravure process parameters such as line screen, ink viscosity, press speed, ESA (Electrostatic Assist) voltage and the air gap at varying levels to evaluate the effect of these process parameters on half-tone mottle. The Stochastic Frequency Distribution Analysis (SFDA) algorithm was used to measure surface properties of paper and half-tone mottle. The experimental data were analysed through ANOVA, main and interaction plot. The results revealed a reduction in mean halftone mottle by 90.48% and 91.25% for 50 GSM and 65 GSM C1S paper respectively. The regression models were developed and validated by conducting additional runs. The results hence obtained shall help to optimize ink transfer and identify the key process variables minimizing half-tone mottle; thereby enhancing the print quality.

Keywords: ANOVA, Coated paper, DOE, Half-tone mottle, Regression models.

1. Introduction

Print quality is measured by attributes such as densitometry, spectrophotometry and print defects such as mottle, missing dots, image sharpness and unevenness in the print gloss. The term print quality is homologous to printability, which is defined as the optimal amalgamation of ink, substrate and process parameters to produce the best quality print.

The ink transfer onto the paper substrate depends on process parameters, ink and substrate properties along with their interactions. These include press speed, nip pressure, Electrostatic Assist (ESA) air gap, ESA voltage, ink viscosity, ink rheology and paper properties such as topography, formation index, roughness, compressibility, electrical properties (surface and volume resistivity for ESA), etc. The variations in these results in non-uniform ink laydown, which leads to half-tone mottle and spoils the look of a printed product. This generates ambiguity in the customer's mind and reduces its selling potential. Thus, these effects need to be measured quantitatively with high precision equipment, to improve print quality. The process cannot be completely impeccable but can be improved. This can be done by meticulously understanding the ESA system and process parameters; as modifying substrate and ink on the press is not within the printer's control.

Gravure process dominates the packaging industry because of its economy for long runs with high print precision. The gravure process includes a gravure cylinder as an image carrier, impression roller, ink fountain and the doctor blade as basic components (Fig. 1). The image carrier is an engraved cylinder, which has image areas in recess and is partially dipped that rotates into an ink duct, thus carrying the ink on to the surface of the cylinder. The excess ink on the cylinder is wiped off by a doctor blade with ink present only in the recessed image cells. An impression roller, a rubber covered roller gives support to the substrate and transfers the ink from the cells to the substrate by capillary action [1]. The process offers excellent print consistency with higher speeds for medium to long runs on a variety of stocks. The major applications of the process are in publication, packaging and speciality printing [2].

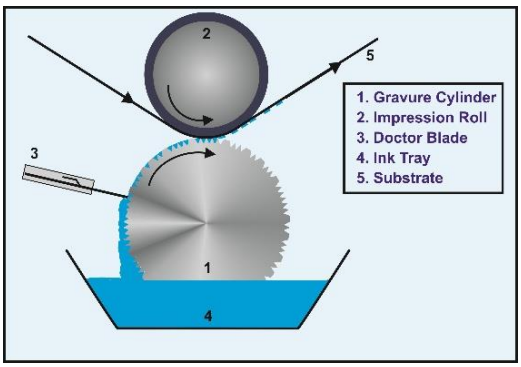

Fig. 1. Gravure printing process.

2. Literature Review

Various instrumental methods have been established in identifying and quantifying such disturbances so as to closely match the visual assessment results. These include STFI band-pass analysis, wavelet and fourier transform and Stochastic

Frequency Distribution Analysis (SFDA). Fahlcrantz et al. [3] studied the influence of mean reflectance over perceived print mottle. The unevenness in print density or non-uniformity in ink transfer is referred to as print mottle. The STFI band-pass analysis (1-8 mm) was employed to calculate the Co-Efficient of Variance (CoV) and a good correlation coefficient (R^2=0.9782) was obtained. Teleman et al. [4] tested the ability of STFI mottling algorithm to calculate mottle over flexo printed linerboard. STFI mottling algorithm employing bandpass analysis was used to analyse scanned images and obtain an instrumental measure of mottle. Visual evaluation was carried out by rating the samples from least to most disturbing by the observers under D50 illumination at 1700 lux. The middle sample was to be assigned a value 100 and the rating for remaining samples was to be assigned proportionally. The instrumental evaluation was done based on standard STFI Mottling CoV 1-8 mm and a correlation (R^2) ranging from 0.69 to 0.95 was achieved. Liu et al. [5] evaluated print mottle over offset papers using Discrete Wavelet Analysis technique. The two-dimensional discrete algorithm removes the noise from the image, which is regarded as mottle index. Moreover, the visual evaluation was carried out by a panel of 10 people with rating 1 as best and 3 as worst. The correlation (R^2) of 0.76 was obtained between instrumental and visual assessment. Rosenberger [6] and Rosenberger et al. [7] described the working of Stochastic Frequency Distribution Analysis (SFDA) algorithm to calculate mottle in a digital image. SFDA maps the average and variation in luminance values of pixels within a target area to calculate back-trap, solid and half-tone mottle index.

The ink transfer is affected by substrate properties, gravure process parameters and ink behaviour. According to Lee and Na [8] and Rentzhog and Fogden [9], the ink transfer increases with a drop in contact angle and surface tension. This further increases the wetting difference between the surface energy of the substrate and surface tension of the ink, thus reducing the mottle. The gravure process parameters such as screen ruling, engraving angle, ink viscosity, impression pressure, doctor blade angle, press speed, hardness and type of resin affect the ink transfer; thereby the print mottle [10-17]. The surface roughness and higher topography index results in missing dots. The dot deformation, missing dots and optical dot gain further lead to higher print mottle [18-24]. The electrostatic assist helps in minimizing the print mottle both in solids and half-tones [25-27].

The evaluation of mean halftone mottle on flexible packaging coated paper using ESA and gravure process parameters have not been addressed. The main objective of this research is to identify significant the gravure process parameters minimizing the half-tone mottle on coated papers, optimizing and validating the optimized settings and checking for its consistency.

3. Materials

3.1. Substrate

The experimental trials were conducted on 50 GSM and 65 GSM C1S paper substrate. The surface energy of the substrate was determined by measuring the contact angle with standard test liquids, i.e., formamide and glycerol. The geometric mean equation was employed to calculate surface energy and was found to be 51.06 mN/m and 48.48 mN/m for 50 GSM and 65 GSM C1S paper respectively. The substrate electrical properties were examined according to ASTM D 257 and ASTM D 149 (Table 1).

Table 1. Properties of paper substrates.

Test	Test method	Unit	50 GSM	65 GSM
Topography	SFDA	Index	10.43	5.23
Paper mottle	SFDA	Index	1.55	1.284
Print Parker Surf (PPS)	T-555 pm-94	µm	0.83	0.79
Insulation resistance	ASTM D 257	MΩ	2000	>2000
Breakdown voltage	ASTM D 149	*V*	900	1100

From Table 1, a higher topography index, mottle index and roughness (PPS) are observed for 50 GSM than 65 GSM. This indicates a better surface for printing on 65 GSM. A higher insulation resistance and breakdown voltage are observed for 65 GSM than 50 GSM. Hence, for a given voltage and air gap, a higher current will be generated for 50 GSM than 65 GSM. The current reduces with increase in the air gap, due to increased resistance of the circuit (Table 2).

Table 2. Current values during printing.

Air gap (mm)	Voltage (kV)	Current (mA)		Resistance (MΩ)	
		50 GSM	65 GSM	50 GSM	65 GSM
1.5	**8**	1.0	0.9	8.00	8.89
	10	1.4	1.3	7.14	7.69
	12	1.7	1.6	7.06	7.50
3	**8**	0.9	0.8	8.89	10.00
	10	1.2	1.1	8.33	9.09
	12	1.6	1.5	7.50	8.00
5	**8**	0.6	0.5	13.33	16.00
	10	0.9	0.8	11.11	12.50
	12	1.3	1.2	9.23	10.00

3.2. Ink

The black Nitrocellulose (NC) ink was employed for printing throughout the experimentation. The ink was diluted with a solvent combination of ethyl acetate, isopropyl alcohol and methoxy propanol in the ratio 5:3:2 to adjust the viscosity being measured by #4 Ford Cup during the press run. The surface tension (γ_l) of ink was 27.95 mN/m as measured by Kyowa Surface Tensiometer.

3.3. Ink-substrate interaction

The contact angles were measured at 17 *sec*, 19 *sec* and 21 *sec* viscosities and interfacial tension (γ_{sl}), work of adhesion (W_a) and spreading coefficient (S) were calculated for 50 GSM and 65 GSM C1S paper using following formulae.

$$\gamma_{sl} = \gamma_s - \gamma_L (\text{Cos } \theta) \quad (1)$$

$$W_a = \gamma_s + \gamma_L - \gamma_{sl} \quad (2)$$

$$S = \gamma_s - \gamma_L - \gamma_{sl} \quad (3)$$

where γ_s=surface tension of paper (51.06 mN/m for 50 GSM and 48.48 mN/m for 65 GSM).

γ_L=surface tension of ink (27.95 mN/m)

Table 3 shows a lower contact angle, interfacial tension and higher work of adhesion at lower viscosity (17 *sec*), thereby resulting in higher spreading coefficient and ink spread. Also for a given viscosity, ink spread (*S*) is more in 50 GSM than 65 GSM.

Table 3. Ink-substrate interaction.

Substrate	Ink viscosity (*sec*)	Contact angle (°)	Interfacial tension (γ_{sl})	Work of adhesion (W_a)	Spreading co-efficient (S)
50 GSM	17	28.42	26.48	52.53	-3.37
	19	31.38	27.20	51.81	-4.09
	21	34.71	28.08	50.93	-4.97
65 GSM	17	30.91	24.50	51.93	-3.97
	19	32.27	24.85	51.58	-4.32
	21	35.84	25.82	50.61	-5.29

3.4. Layout design

The layout design (Fig. 2) comprises an image, logo, normal and reverse text, step wedge and half-tone patch. The cylinder was electronically engraved with compressed cells. The printed half-tone area was scanned at an area of interest of 70 mm × 55 mm (dotted lines) with Epson V700 scanner at 1200 ppi resolution. The scanned images were processed through the SFDA algorithm to calculate the mean halftone mottle index.

Fig. 2. Layout design.

3.5. Experimental process

A general full factorial design of experiment (DOE) was generated with 5 factors viz., line screen, viscosity, speed, ESA voltage and air gap with 2 replicates, thus a total of 216 runs (Table 4). The baseline for half-tone mottle was defined by conducting production runs for few days on 4-colour pilot gravure printing machine on both 50 GSM and 65 GSM substrates. The production runs were conducted at 65 l/cm line screen, 19 *sec* ink viscosity as measured by #4 Ford Cup, 3.5 kg/cm^2 pressure and 1.667 m/s speed without ESA. The data was collected from 20 printed sheets being considered as sample size. The sample size was calculated based on the 1-sample t-test. The calculated power values above 0.9 confirmed the adequacy

of the sample size. The data collected from the production run showed mean halftone mottle index as 126.01 and 95.98 for 50 GSM and 65 GSM C1S paper, hence considered as a baseline. The printed halftone area (30%) was scanned with Epson V700 scanner at 1200 ppi resolution and evaluated by Verity IA Print Target v3 software, which employs SFDA algorithm technique. The scanned images were analysed with an area of interest (AOI) of 70 mm × 55 mm marked in dotted line (Fig. 2). SFDA measures the rate of change in luminance value from a two-dimensional scanned image. It interprets the scanned image with recorded luminance value, which evaluates the uniformity of ink transfer on the substrate surface being represented by an index value. Higher the mottle index number, more is the uneven ink lay down. The experimental runs were analysed by analysis of variance (ANOVA), main and interaction plots to identify the optimal settings. The optimal results were verified and the regression models were developed and validated by conducting additional runs.

Table 4. Process variables and levels.

S. No.	Variables	Unit	Levels		
			Low	mid	High
1	Line screen	l/cm	60	-	65
2	Viscosity	*sec*	17	19	21
3	Speed	m/s	1.33	-	2
4	Voltage	kV	8	10	12
5	Air gap	mm	1.5	3	5

4. Results and Discussion

4.1. Dot structure analysis

The printed dots were captured by DIGITUS Microscope at 220X zoom on 50% patch to check for dot reproduction and circularity.

The dot structure analysis (Figs. 3 and 4) show more dot spread at lower viscosity (17 *sec*) than higher viscosity (21 *sec)* for both 50 GSM and 65 GSM C1S paper. The circularity of dot refers to the roundness and is an indicator of dot reproduction. The dot circularity is equal to 1 for a circle. The closer to 1, better the circularity and quality of printed dot. The dot circularity increased with increase in viscosity from 17 s to 19 s (0.68 to 0.71) for 50 GSM and (0.69 to 0.72) for 65 GSM C1S paper. However, at 21 s the circularity reduced to 0.67 and 0.69 for 50 GSM and 65 GSM respectively. This is due to the cell clogging that led to lack of ink transfer from gravure cell on to the paper. The dot circularity improved with increase in voltage from 8 kV to 10 kV (0.67 to 0.70) for 50 GSM and (0.68 to 0.72) for 65 GSM. The dot circularity at 12 kV reduced to 0.68 for 50 GSM and 0.70 for 65 GSM respectively. The electrostatic force is insufficient to pull ink from the gravure cell thus, resulting in fisheye effect dots at 8 kV voltage and 5 mm air gap for both 50 GSM and 65 GSM (Figs. 5-8). On the other hand, dot distortion is observed at 12 kV voltage and 1.5 mm air gap for both the substrates. This is due to the higher current that was responsible for ink immobilization and uneven dot spread. The dot reproduction improved at an intermediate level of viscosity (19 *sec*), voltage (10 kV) and air gap (3 mm) and more uniform on 65 GSM due to lower surface undulations than 50 GSM.

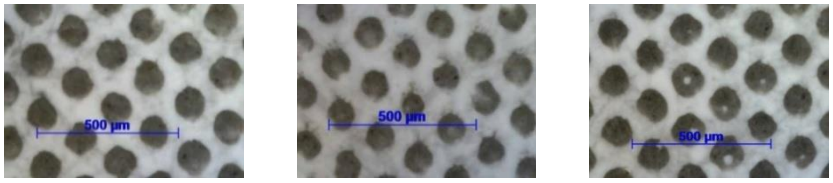

(a) 17 s. **(b) 19 s.** **(c) 21 s.**

Fig. 3. Dot structures on 50 GSM.

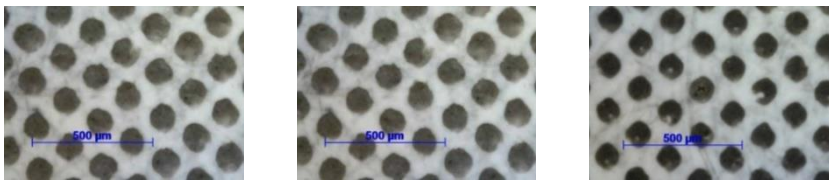

(a) 17 s. **(b) 19 s.** **(c) 21 s.**

Fig. 4. Dot structures on 65 GSM.

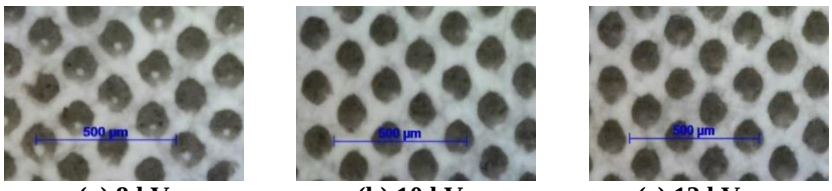

(a) 8 kV. **(b) 10 kV.** **(c) 12 kV.**

Fig. 5. Dot structures on 50 GSM.

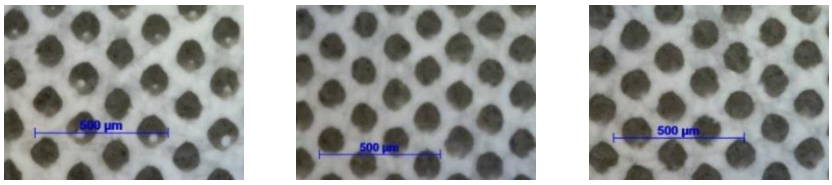

(a) 8 kV. **(b) 10 kV.** **(c) 12 kV.**

Fig. 6. Dot structures on 65 GSM.

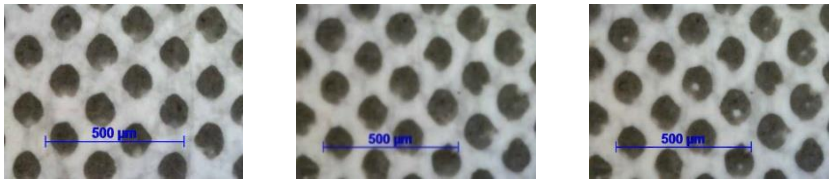

(a) 1.5 mm. **(b) 3 mm.** **(c) 5 mm.**

Fig. 7. Dot structures on 50 GSM.

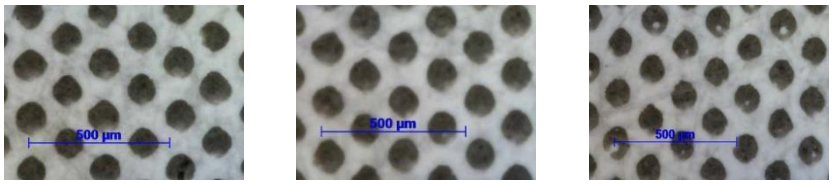

(a) 1.5 mm. **(b) 3 mm.** **(c) 5 mm.**

Fig. 8. Dot structures on 65 GSM.

4.2. Main effects

The main effects plot (Fig. 9) indicates a reduction in mean halftone mottle index at higher line screen and speed with intermediate levels of viscosity, ESA voltage and air gap. The increase in line screen at 65 l/cm reduces the cell opening thereby reducing the amount of ink transfer. This leads to lower ink spreading with sharper edges thus, reducing mean halftone mottle index. The ink spread is highest at lower viscosity (17 *sec*) due to lower solid content and higher spreading coefficient (Table 3), thus resulting in higher mean halftone mottle. With the increase in viscosity (19 *sec*) ink spread reduces thus lowering mean halftone mottle. However, with a further rise in viscosity (21 *sec*), the evaporation of the solvent in the gravure cell leads to cell clogging.

This result in inadequate ink transfer leading to non-uniform ink transfer from the cells; thereby increased half-tone mottle. Moreover, the rise in centrifugal force with increasing press speed significantly increases ink evacuation, thereby lowering mean halftone mottle. The decrease in voltage (8 kV) and an increase in air gap (5 mm) results in non-uniform ink transfer. The uneven ink transfer results in uneven ink absorption and thereby increasing mean halftone mottle. However, ink immobilization results with the rise in current at a higher voltage (12 kV) and lower air gap (1.5 mm). This leads to deterioration in dots thereby increasing mean halftone mottle. The electrical properties of the substrate also influence mottle in halftones. The current flowing through the circuit is higher due to lower insulation resistance and break down voltage in 50 GSM. This results in increased distortion spread and higher mean halftone mottle index in 50 GSM than 65 GSM.

4.3. Interaction plot

The interaction plots (Fig. 10) indicated lower mean halftone mottle at 65 l/cm line screen, 19 *sec* viscosity, 2 m/s press speed, 10 kV ESA voltage and 3 mm air gap for both 50 GSM and 65 GSM C1S paper. A considerable interaction is observed between viscosity and air gap in mean halftone mottle. The ink transfer increases at lower viscosity (17 *sec)* at lower air gap (1.5 mm) but the dot distorts due to higher electrostatic force developed at the printing nip, thereby increasing mean halftone mottle. On the other hand, fisheye pattern is observed at higher viscosity (21 *sec*) and air gap (5 mm). This is due to insufficient electrostatic pull and higher viscous drag in the ink, which reduces capillary force during ink transfer. At 19 s*ec* viscosity and 3 mm air gap, ink spreading is controlled that led to reduced mean halftone mottle. At higher press speed (2 m/s) and lower air gap (1.5 mm), higher centrifugal force and the electrostatic force are generated. This leads to increased ink transfer and immobilization on the substrate thereby increasing mean halftone mottle. The same phenomenon is observed at higher voltage and lower air gap thereby increasing mean halftone mottle.

4.4. Analysis of Variance (ANOVA)

The ANOVA Tables 5 and 6 signifies that all the main effects significantly affect mean halftone mottle as the p-value was below the significance level (0.05). The line screen and second degree of viscosity, ESA voltage and air gap were the significant factors affecting mean halftone mottle. The interactions between press speed and air gap effect mean halftone mottle notably. The R^2 indicates that 94.78%

and 96.72% of the variability is explained by both the models with 96.30% and 94.78% predictive ability for 50 GSM and 65 GSM respectively. The R^2 (adj) of 95.17% and 96.54% signifies sufficient regression by the use of five factors for 50 GSM and 65 GSM paper. The lack-of-fit with p-value above 0.05 indicates adequacy of models for both the substrates.

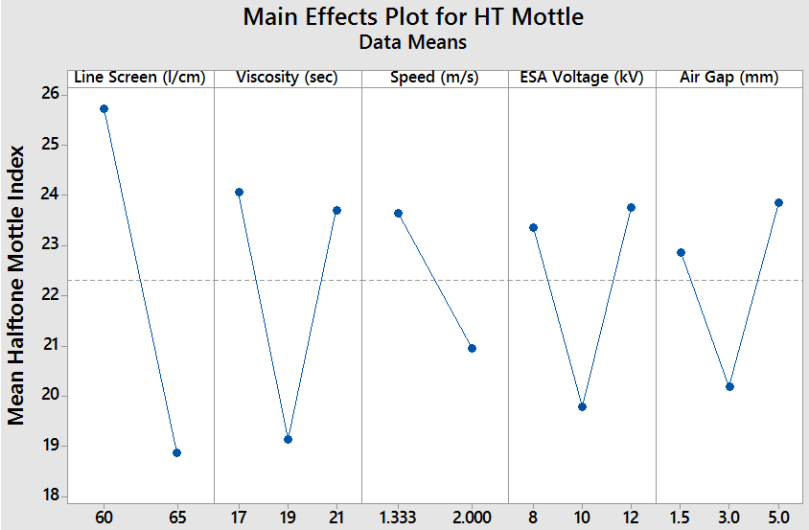

(a) 50 GSM.

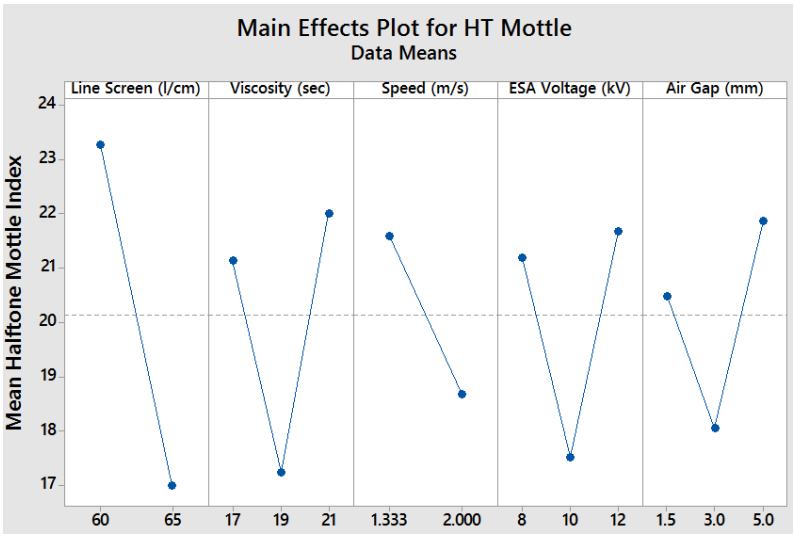

(b) 65 GSM.

Fig. 9. Main effects of mean halftone mottle index.

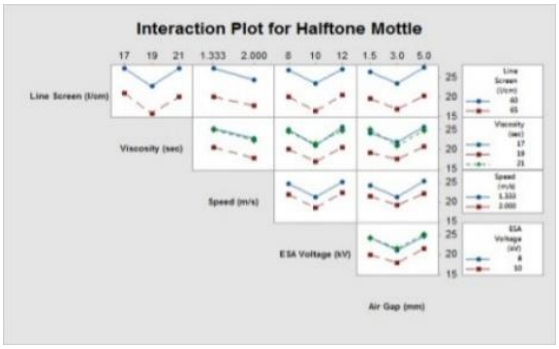

(a) 50 GSM.

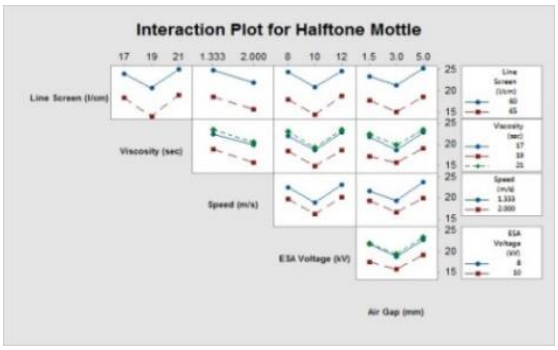

(b) 65 GSM.

Fig. 10. Interaction of mean halftone mottle index.

Table 5. ANOVA table for regression of mean halftone mottle-50 GSM.

Source	DF	Adjusted SS	Adjusted MS	F-value	P-value
Regression	12	5285.41	440.25	353.77	0.000
Line screen (l/cm)	1	2551.38	2551.38	2049.27	0.000
Viscosity (*sec*)	1	4.95	4.95	3.98	0.047
Speed (m/s)	1	394.63	394.63	316.97	0.000
ESA voltage (kV)	1	6.01	6.01	4.83	0.029
Air gap (mm)	1	5.47	5.47	4.39	0.037
Viscosity (*sec*)* Viscosity (*sec*)	1	1079.14	1079.14	866.77	0.000
ESA voltage (kV)* ESA voltage (kV)	1	686.93	686.93	551.77	0.000
Air gap (mm)* Air gap (mm)	1	460.49	460.49	369.87	0.000
Line screen (l/cm)* Viscosity (*sec*)	1	8.55	8.55	6.86	0.009
Line screen (l/cm)* Speed (m/s)	1	6.08	6.08	4.88	0.028
Viscosity (*sec*)* Air gap (mm)	1	20.57	20.57	6.52	0.000
Speed(m/s)* Air gap (mm)	1	5.53	5.53	4.44	0.036
Error	203	252.74	1.25		
Lack of git	95	125.53	1.32	1.12	0.281
Pure error	108	127.21	1.18		
Total	215	5538.15			

Summary of model

S=1.11580 *R*-sq=95.44%

R-sq (adjusted)=95.17% *R*-sq (predictive)=94.78%

Regression equation for mean halftone mottle in 50 GSM.

$$Halftone\ Mottle = 593.8 - 0.784\ Line\ Screen - 41.67\ Viscosity - 15.57\ Press\ Speed - 18.81\ ESA\ Voltage - 3.39\ Air\ Gap + 1.1854\ Viscosity * Viscosity + 0.9457\ ESA\ Voltage * ESA\ Voltage + 1.0360\ Air\ Gap * Air\ Gap - 0.0487\ Line\ Screen * Viscosity + 0.2012\ Line\ Screen * Press\ Speed - 0.1318\ Viscosity * Air\ Gap - 0.335\ Press\ Speed * Air\ Gap \quad (4)$$

Table 6. ANOVA table for regression of mean halftone mottle-65 GSM.

Source	DF	Adjusted SS	Adjusted MS	F-value	P-value
Regression	11	4824.9	438.6	547.07	0.000
Line screen (l/cm)	1	2127.5	2127.5	2653.5	0.000
Viscosity (*sec*)	1	26.8	26.84	33.48	0.000
Speed (m/s)	1	454.5	454.49	566.9	0.000
ESA voltage (kV)	1	8.42	8.42	10.51	0.001
Air gap (mm)	1	22.29	22.29	27.80	0.000
Viscosity (*sec*)* Viscosity (*sec*)	1	901.41	901.41	112.27	0.000
ESA voltage (kV)* ESA voltage (kV)	1	738.14	738.14	920.63	0.000
Air gap (mm)* Air gap (mm)	1	434.31	434.31	541.69	0.000
Line screen (l/cm)* ESA voltage (kV)	1	3.24	3.24	4.04	0.046
Line screen (l/cm)* Air gap (mm)	1	8.67	8.67	10.82	0.001
Speed (m/s)* Air gap (mm)	1	19.38	19.38	24.17	0.000
Error	204	163.56	0.80		
Lack of fit	96	88.11	0.92	1.31	0.084
Pure error	108	75.45	0.70		
Total	215	4988.4			

Summary of model

S=0.895419 *R*-sq = 96.72%

R-sq (adjusted)=96.54% *R*-Sq (predictive) = 96.30%

Regression equation for mean halftone mottle in 65 GSM

$$Halftone\ Mottle = 595.8 - 1.378\ Line\ Screen - 40.95\ Viscosity - 2.366\ Press\ Speed - 21.36\ ESA\ Voltage - 1.60\ Air\ Gap + 1.0834\ Viscosity * Viscosity + 0.980\ ESA\ Voltage * ESA\ Voltage + 1.006\ Air\ Gap * Air\ Gap + Line\ Screen * ESA\ Voltage - 0.056\ Line\ Screen * Air\ Gap - 0.626\ Press\ Speed * Air\ Gap \quad (5)$$

4.5. Verification and consistency

The minimum mean halftone mottle was observed at 65 lpcm line screen, 19 *sec* viscosity, 2 m/s speed, 10 kV voltage and 3 mm air gap, hence considered as best settings. These settings were rerun and checked for its consistency.

From Table 7, a significant reduction in half-tone mottle by 90.48% and 91.25% is observed from production to consistency run for 50 GSM and 65 GSM paper.

Table 7. Production, verification and consistency of mean halftone mottle.

Trials	50 GSM		65 GSM	
	Mean halftone mottle	Standard deviation	Mean halftone mottle	Standard deviation
Production run	126.01	7.3971	95.98	9.7918
Verification run	12.02	1.1577	8.62	1.1577
Consistency run	12.00	1.2992	8.40	1.3184

4.6. Validation

The models were validated by comparing the actual mean halftone mottle index values obtained through experimentation with the calculated mottle values from the regression of Eqs. (4) and (5).

The scatter plot (Fig. 11) illustrates that actual and predicted values lie in close proximity with correlation coefficients of 0.944 and 0.927 for 50 GSM and 65 GSM. This indicates a good predictive ability of the developed regression models.

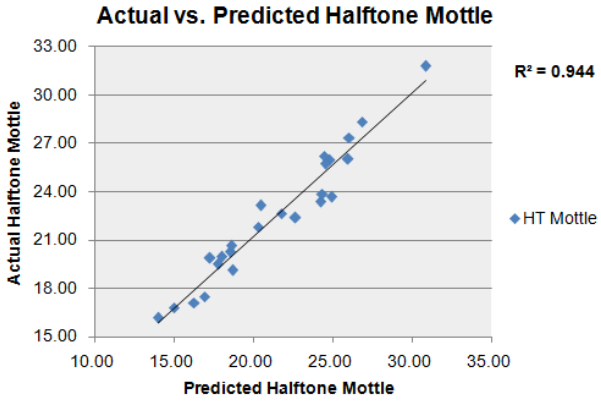

(a) 50 GSM.

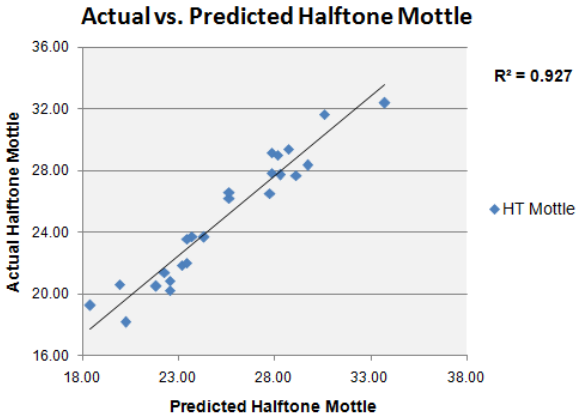

(b) 65 GSM.

Fig. 11. Actual vs. predicted mottle.

5. Conclusions

An investigation of halftone mottle on coated papers was carried out by varying gravure process parameters. The evaluation was done using statistical analytical methods. Some concluding observations from the investigation are given as follows.

- The main factors such as line screen, air gap, viscosity, speed and voltage were significant in minimizing half-tone mottle index.
- The half-tone print mottle was minimized at 65 l/cm line screen, 19 *sec* viscosity, 1.667 m/s speed 10 kV voltage and 3 mm air gap for 50 GSM and 65 GSM respectively.
- The second degree of viscosity, ESA voltage and air gap was also important in mean half-tone mottle reduction.
- The regression models were developed and validated to predict the mean halftone mottle index. The mean halftone mottle index was reduced by 90.48% and 91.25% for 50 GSM and 65 GSM respectively.
- The print defects such as half-tone mottle lead to rejections thereby suffering heavy wastage of ink, substrate, packing and transportation cost, thus damaging the environmental sustainability. Thus, identifying the optimal settings obtained shall assist printers, ink and paper manufacturers to make necessary changes in production.

Nomenclatures

I	ESA current, mA
IR	Insulation resistance, MΩ
l/cm	Line screen of engraved gravure cylinder
PPS	Parker print surf roughness, µm
S	Spreading coefficient
sec	Ink viscosity as measured by #4 Ford Cup
V	ESA voltage, kV
W_a	Work of adhesion
γ_l	Surface tension of ink, mN/m
γ_s	Surface tension of solid, mN/m
γ_{sl}	Interfacial tension between solid and liquid

Greek Symbols

θ	Contact angle, deg.

Abbreviations

ANOVA	Analysis of Variance
ASTM	American Standard Testing Method
DOE	Design of Experiments
ESA	Electrostatic Assist
GSM	Gram per Square Meter
NC	Nitrocellulose Ink
SFDA	Stochastic Frequency Distribution Analysis

References

1. Gravure Association of Americas Inc. and Gravure Education Foundation. (2003). *Gravure process and technology (2nd ed.)*. New York: Gravure Association of America.
2. Kipphan, H. (2001). *Handbook of print media: Technologies and production methods*. Germany: Springer-Verlag, Berlin Heidelberg.
3. Fahlcrantz, C.-M.; Johansson, P.-A.; and Aslund, P. (2003). The influence of mean reflectance on perceived print mottle. *Journal of Imaging Science and Technology*, 47(1), 54-59.
4. Teleman, A.; Christiansson, H.; Johansson, P.-A., Fahlcrantz, C.-M.; and Lindberg, S. (2005). Correct measurements of half-tone print mottle on flexo printed linerboard. *STFI-Packforsk.* Report No. 39.
5. Liu, G.D.; Zhang, M.Y.; and Liang, Q.P. (2013). Study on the assessment method of print mottle using discrete wavelet analysis. *Applied Mechanics and Materials*, 262, 177-180.
6. Rosenberger, R.R. (2003). Stochastic frequency distribution analysis as applied to mottle measurement. Retrieved September 2017, from http://3jg1wh1bi3pi4b0p323yv9o5.wpengine.netdna-cdn.com/wp-content/uploads/2015/11/stochastic-frequency.pdf.
7. Rosenberger, R.; Clark, D.; and Drake, D. (2001). Back-trap and half-tone mottle measurement with stochastic frequency distribution analysis. Retrieved September 2017, from http://www.verityia.com/wp-content/uploads/2015/11/mottle.pdf.
8. Lee, S.; and Na, Y. (2010). Analysis on the ink transfer mechanism in R2R application. *Journal of Mechanical Science and Technology*, 24(1), 293-296.
9. Rentzhog, M.; and Fogden, A. (2006). Print quality and resistance for water-based flexography on polymer-coated boards: Dependence on ink formulation and substrate pre-treatment. *Progress in organic coatings*, 57(3), 183-194.
10. Stancic, M.; Novakovic, D.; Tomic, I.; and Karlovic, I. (2012). Influence of substrate and screen thread count on reproduction of image elements in screen printing. *Acta Graphica*, 23(1-2), 1-12.
11. Bohan, M.F.J.; Claypole, T.C.; and Gethin, D.T. (1998). An investigation into ink transfer in rotogravure printing. Retrieved September 2017, from https://www.printing.org/taga-abstracts/an-investigation-into-ink-transfer-in-rotogravure-printing.
12. Bohan, M.F.J.; Claypole, T.C.; and Gethin, D.T. (2000). The effect of process parameters on product quality of rotogravure printing. *Proceedings of the Institution of Mechanical Engineers, Part B: Journal of Engineering Manufacture*, 214(3), 205-219.
13. Deng, P.J.; Fang, W.; and Lu, J.D. (2014). Study about influencing of printing process on gravure printing ink transfer. *Applied Mechanics and Materials*, 469, 301-304.
14. Deng, P.J.; Zhang, G.M.; Wang, Y.; and Fang, W. (2011). Influence of screen ruling and engraving needle tip angle on ink transfer for gravure. *Advanced Materials Research, Printing and Packaging Study*, 174, 215-218.

15. Elsayad, S.; Morsy, F.; El-Sherbiny, S.; and Abdou, E. (2002). Some factors affecting ink transfer in gravure printing. *Pigment and Resin Technology*, 31(4), 234-240.
16. Olsson, R.; Yang, L.; Stam, J.v.; and Lestelius, M. (2007). Effects of elevated temperature on flexographic printing. *Proceedings of the 34th IARIGAI International Research Conference of Advances in Printing and Media Technology.* Grenoble, France, 1-9.
17. Gencoglu, E.N. (2005). The effects of some engraving and film substrate parameters on the solid density and the dot gain in gravure printing. *Surface Coatings International Part B: Coatings Transactions*, 88(1), 19-23.
18. Sprycha, R.; Durand Jr., R.; and Pace, G. (2007). Mechanisms of abnormal dot deformation in gravure printing. Retrieved September 2017, from https://www.printing.org/taga-abstracts/t070482.
19. Kawasaki, M.; Ishisaki, M.; and Yoshimoto, Y. (2009). Investigation into the cause of print mottle in halftone dots of coated paper: Effect of optical dot gain non-uniformity. *Japan Tappi Journal*, 63(11), 1362-1373.
20. Laurent, G.G. (2002). *Measurement and prediction procedures for printability in flexography* (MP3 flexo). Ph.D. Thesis. Department of Numerical Analysis and Computer Science, Royal Institute of Technology, Stockholm, Sweden.
21. Velho, J.; and Santos, N. F. (2010). Surface topography of coated papers: From the evaluation process to the quality improvement. *Material Science Forum*, 636-637, 977-984.
22. Koyamoto, H.; and Okomori, K. (2007). Effect of surface properties of base paper on print quality. *Japan Tappi Journal*, 61(4), 470-476.
23. Martorana, E.; Zeigler, H.; Campo, F.W.A.; and Juhe, H.-H. (2006). Causes of missing dots in rotogravure printing. *Wochenblatt für Papierfabrikation*, 62(12), 722-728.
24. Bohlin, E.; Lestelius, M.; and Johansson, C. (2013). Flexographic ink-coating interactions-Effects of porous structure variations of coated paperboard, *Nordic Pulp & Paper Research Journal*, 28(4), 573-581.
25. Joshi, A.V.; Dettke, C.; and Steingraeber, J. (2016). Investigation of electrostatic assist on solid mottle reduction for shrink films. *Journal of Coatings Technology and Research*, 13(2), 375-383.
26. Joshi, A.V.; and Bandyopadhyay S. (2015). Effect of ink transfer on print mottle in shrink films. *Journal of Coatings Technology Research*, 12(1), 205-213.
27. Rong, X.; Pekarovic, J.; and Pekarovicova, A. (2004). Gravure printability from laser and electromechanically engraved cylinder. *Proceedings of the International Printing and Graphic Arts Conference*. Vancouver, Canada, 151-154.